Modification of mesoporous silicate SBA-15 with tris[bis(trimethylsilyl)amido]samarium and its utility in Tishchenko reaction

Yinghua Chen [a], Zhenyu Zhu [a], Jie Zhang [a], Jianzhong Shen [a], Xigeng Zhou [a,b,*]

[a] *Department of Chemistry, Molecular Catalysis and Innovative, Material Laboratory, Fudan University, Handan Road 220, Shanghai 200433, People's Republic of China*
[b] *State Key Laboratory of Organometallic Chemistry, Shanghai 200032, People's Republic of China*

Abstract

Treatment of mesoporous silicate SBA-15 with $Sm[N(SiMe_3)_2]_3$ led to the formation of a novel organolanthanide/inorganic hybrid material $[SBA-15]Sm[N(SiMe_3)_2]_x$ via abstraction of $N(SiMe_3)_2$ by terminal silanol groups and subsequent surface silylation. The hybrid material was characterized by elemental analyses, IR spectroscopy, X-ray diffraction, and nitrogen sorption, indicating a successful tailoring inside the silicate SBA-15 and the maintenance of the well-ordered mesostructure. This hybrid material is a promising heterogeneous catalyst for the Tishchenko reaction, where it is superior to the homogeneous correspondent in deactivation behavior, reusability and relative tolerance to oxygen, particularly in the control of selectivity of mixed Tishchenko reaction due to the steric hindrance and the diffusion control derived from the surface confinement.
© 2005 Elsevier B.V. All rights reserved.

Keywords: Organolanthanide; Tishchenko reaction; SBA-15; Immobilization

1. Introduction

There is currently considerable interest in studying heterogenization of homogeneous catalysts for advantageous recovering and recycling them from reaction system [1]. Of particular interest has been the exploration of immobilization of these homogeneous catalysts onto porous inorganic solids to create organic–inorganic hybrid catalysts. Grafting the organolanthanide catalysts onto porous silica materials by heterogeneously performed silylamide route [2] proved to be an appealing way to the heterogenization of homogeneous catalysts.

For example, it has been found that some organolanthanide catalysts can be grafted onto MCM-41 in terms of the remaining catalytic activity and the spatial restriction of mesopores can lead to high stereoselectivity of the products [3]. As a new mesoporous material, SBA-15 [4] is possessed of a two dimension hexagonal pore structure, its texture with larger pore diameter and pore volume compared to MCM-41 means more flexibility in guest loading and less risk of the pore blockage [5], which may ensure the attack of the substrates on the active sites. The potential of such a structurally ordered silica material to act as a versatile support material has previously been demonstrated by SBA-15-grafted organic moieties, inorganic complexes and organotransition metal species [6], intriguing our great interest of the corresponding immobilization of organolanthanides onto this material.

---

* Corresponding author. Tel.: +86 216 564 3769; fax: +86 216 564 1740.
E-mail address: xgzhou@fudan.edu.cn (X. Zhou).

The Tishchenko reaction is one of the most attractive transformations of aldehydes, and the search for cheaper and more effective catalysts is a current interest [7–9]. Recently, lanthanide silylamide complexes $Ln[N(SMe_3)_2]_3$ have proved to be one of the most active catalysts for Tishchenko reaction [10], but their weakness for the oxygen and water-sensitivity and nonreusability impedes them from the application in the industry. Therefore, it would be of great interest to determine whether the immobilization of lanthanide bis(trimethylsily)amides onto the SBA-15 could yield the hybrid materials which are not only active in the Tishchenko reaction, but can be conveniently recovered from reaction environments. Herein, we report the first $Sm[N(SiMe_3)_2]_3$-modified SBA-15 material and its catalytic studies in Tishchenko reaction.

2. Results and discussion

2.1. Synthesis and characterization of the hybrid material

The SBA-15 material used in this study was synthesized by employing nonionic block copolymer P123 as a template described previously [11] and dehydrated at $200\,°C/10^{-3}$ mbar for 8 h prior to use. The immobilizing procedure is readily carried out by the direct reaction of SBA-15 and $Sm[N(SiMe_3)_2]_3$ in hexane at ambient temperature for several days (Scheme 1). The liberated silylamine can further react with the residual silanol groups and passivate them, which is consistent with the previous observation [12] and is in favor of decreasing the side reactions in catalysis [13] and improve the hydrophobicity of the hybrid material [14]. The hybrid material $[SBA-15]Sm[N(SiMe_3)_2]_x$(S2) was characterized by elemental analyses, IR spectroscopy, X-ray diffraction and nitrogen sorption, indicating a successful tailoring inside the silicate SBA-15 and the maintenance of the well-ordered mesostructure.

As shown in Fig. 1, both S1 and S2 display a framework bands for the v_{as}(Si–O–Si) at $1080\,cm^{-1}$ and a strong peak at $804\,cm^{-1}$ attributable to v_{sym}(Si–O–Si). The considerable weakening of the relative intensity of

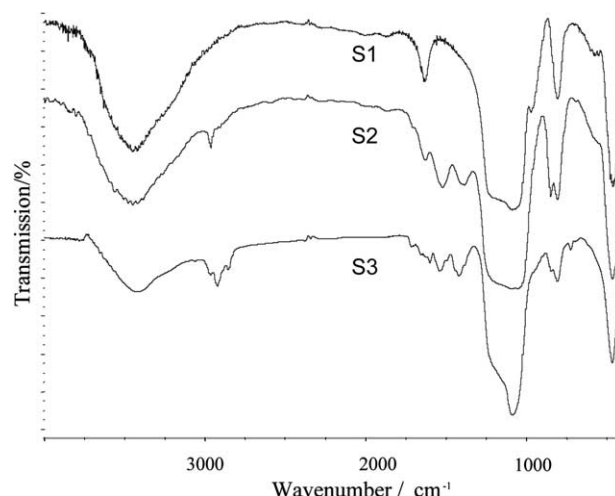

Fig. 1. The FT-IR spectra of SBA-15 (S1), hybrid material (S2) and recovered material (S3).

the absorption band at $3442\,cm^{-1}$ assigned to the hydrogen bound silanols from S1 to S2 demonstrates a part consumption of the silanol groups. The presence of the trimethylsilyl moieties in S2 is characterized by the appearance of three new peaks at 2964, 1392 and $846\,cm^{-1}$.

Fig. 2 shows the XRD patterns of the host material S1 and the hybrid material S2. For S1, the observation of four diffraction peaks that can be indexed to (100), (110), (200), and (210) reflections indicates a well-ordered two-dimensional (2D) mesostructure. The introduction of the $Sm[N(SiMe_3)_2]_3$ results in the reduction of the (100) and (110) reflections and the disappearance of the (200) and (210) reflections. This suggests that the intensity reduction may be a consequence of the contrast matching between the silicate wall and the organic moieties in the cavities [15]. But the observance of (100) and (110) peaks indicates the intact of the well-ordered mesoporous structure. From the wide-angle XRD pattern of the S2 material, only a broad XRD reflection peak derived from the diffraction of the amorphous wall of the material is displayed, which implies a molecular-lever disposal of the $Sm[N(SiMe_3)_2]_3$ on the internal surface.
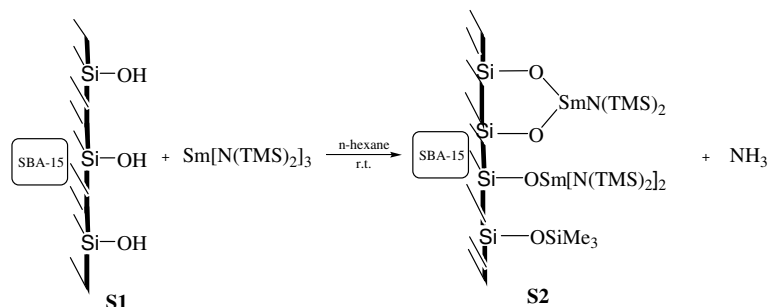
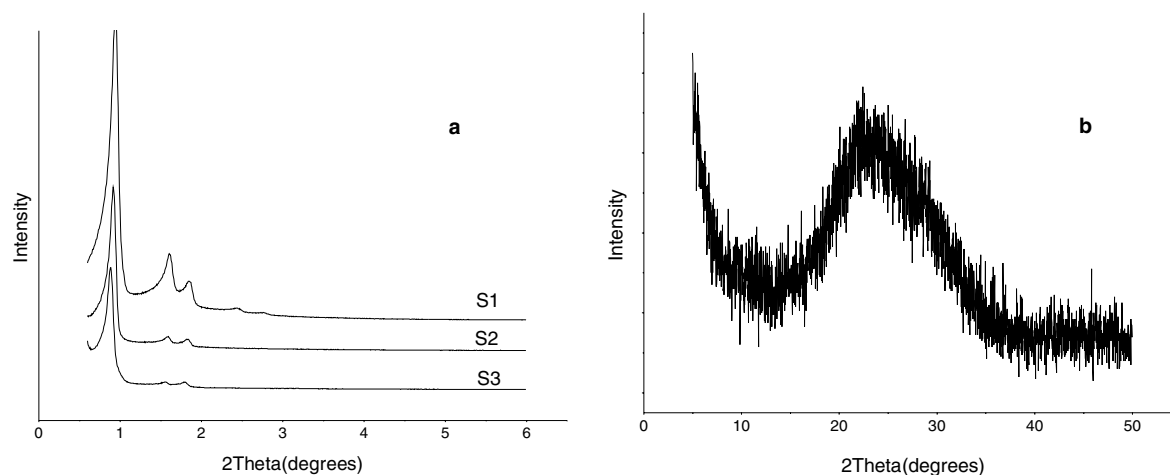Scheme 1. Immobilization of $Sm[N(SiMe_3)_2]_3$ onto mesoporous SBA-15.

Fig. 2. The small-angle powder XRD patterns of **S1**, **S2** and **S3** (a) and wide-angle powder XRD pattern of **S2** (b).

The success of the introduction of $Sm[N(SiMe_3)_2]_x$-moiety onto the SBA-15 is also confirmed by the N_2 adsorption–desorption isotherms for **S1** and **S2**. Both samples show type IV isotherm with a H1 hysteresis loop, characteristic of mesoporous materials according to the IUPAC classification. The parent material **S1** indicates a significant increment for the absorption of N_2 between the relative pressures 0.65 and 0.70. The hysteresis above the relative pressures 0.65 can be attributed to the capillary condensation. The incorporation of $Sm[N(SiMe_3)_2]_x$-moiety is characteristic in the isotherm for its lower uptake of N_2 and earlier onset of hysteresis compared to the parent material. The calculated BET surface areas and the pore diameter according to the Barrett–Joyner–Halenda (BJH) method also show the difference between the host material **S1** and modified material **S2**, the latter displays a significant drop in the two indexes. Noticeably, the preservation of the type IV isotherm is contrast to the observation in introduction of silylamides into the MCM-41 [16], which gave only the type I isotherm. From Fig. 2, we can also find that **S2** exhibits a narrow pore size distribution similar to **S1**, reflecting that $Sm[N(SiMe_3)_2]_x$-moiety is uniformly dispersed inside the channel.
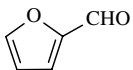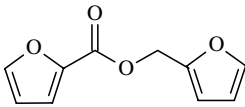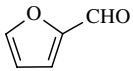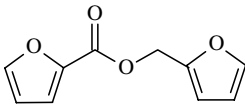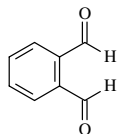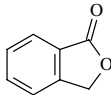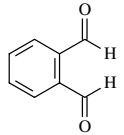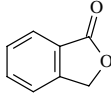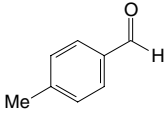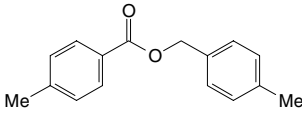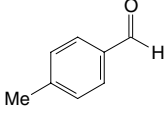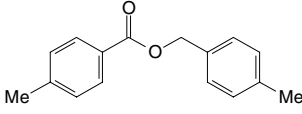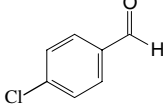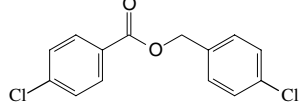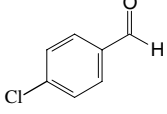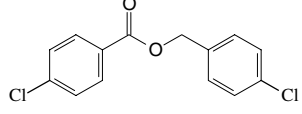
2.2. Catalytic activity in Tishchenko reaction

In order to elucidate whether the grafting process for silylamides is practically necessary, and what advantages it offers, we examined the parallel catalytic performances of $Sm[N(SMe_3)_2]_3$ and $[SBA-15]Sm[N(SMe_3)_2]_x$ in Tishchenko reaction. All the catalytic reactions were carried out at ambient temperature and the catalysts (2.5 mol% metal) were dissolved or suspended in the solvents, respectively. Main results are summarized in Table 1. A comparison of homogeneous and heterogeneous catalysis demonstrates that the reaction rate in **S2** cata-

lytic system is slightly slower than that in the corresponding homogeneous system due to the restricted diffusion. For example, the yields are significantly lower than those in the homogeneous cases when the **S2**-catalyzed reactions are also quenched in 24 h. However, the final yields are comparable to those in the homogeneous cases upon prolonged reaction time. The poor yields of the entries 11 and 12 may be attributed to the deactivation of the +M effect of the substituted phenyl on the carbonyl and the inherent steric hindrance of the substrate. Significantly, if butyl aldehyde was applied, the **S2** catalytic system gives a different selectivity of products from the homogeneous system. Trimers are generated as the main products in the heterogeneous system, while a complex mixture of oligomers is observed under the same conditions in the homogeneous one (Scheme 2). This difference might be partly contributed to the surface or pore confinement of the hybrid material which disfavors the further aggregation of the trimeric intermediates with other aldehyde molecules.

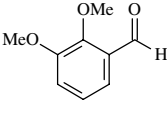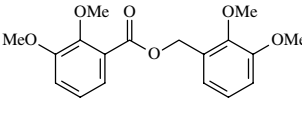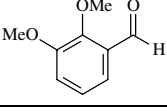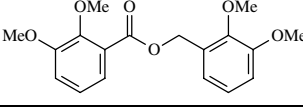The hybrid material displays greater stability to oxygen compared with $Sm[N(SMe_3)_2]_3$. The manipulations involved the heterogeneous catalytic reactions allow to be performed without the protection of N_2 for a short time, while the same procedure for $Sm[N(SMe_3)_2]_3$ is unfeasible. Moreover, the hybrid material is easily separated from the reaction mixture by centrifugation and can be reused. In most of the cases, the recovered materials keep basically the inherent activity in a second or third catalytic run (Table 1). In contrast to the zeolite-based organic transformation where the pore blockage was usually observed [17], X-ray diffraction and nitrogen sorption analyses shows that the recovered material (S3) from entry 2 maintains a well-ordered mesostructure and the same pore diameter with S2, indicating that the pore blockage in these catalytic processes does not occur under involved conditions due to the large pore

Table 1
Tishchenko reactions catalyzed by Sm[N(SiMe$_3$)$_2$]$_3$ and hybrid material (S2)

Entry	Catalyst	Substrate	Time (h)	Procuct	Yield (%)[a]
1.	Sm[N(SiMe$_3$)$_2$]$_3$	PhCHO	24	PhCOOCH$_2$Ph	85
2.	S2	PhCHO	48	PhCOOCH$_2$Ph	80(1st run) 70(2nd run) 50(3rd run)
3.	Sm[N(SiMe$_3$)$_2$]$_3$	furfural (furan-2-CHO)	24	furan-2-COOCH$_2$-furan	45
4.	S2	furfural (furan-2-CHO)	48	furan-2-COOCH$_2$-furan	30(1st run) 30(2nd run) 16(3rd run)
5.	Sm[N(SiMe$_3$)$_2$]$_3$	phthalaldehyde (benzene-1,2-diCHO)	24	phthalide (isobenzofuran-1(3H)-one)	100
6.	S2	phthalaldehyde (benzene-1,2-diCHO)	48	phthalide (isobenzofuran-1(3H)-one)	100(1st run) 95(2nd run) 92(3rd run)
7.	Sm[N(SiMe$_3$)$_2$]$_3$	4-Me-C$_6$H$_4$-CHO	24	4-Me-C$_6$H$_4$-COOCH$_2$-C$_6$H$_4$-4-Me	82
8.	S2	4-Me-C$_6$H$_4$-CHO	48	4-Me-C$_6$H$_4$-COOCH$_2$-C$_6$H$_4$-4-Me	78(1st run) 75(2nd run) 54(3rd run)
9.	Sm[N(SiMe$_3$)$_2$]$_3$	4-Cl-C$_6$H$_4$-CHO	24	4-Cl-C$_6$H$_4$-COOCH$_2$-C$_6$H$_4$-4-Cl	85
10.	S2	4-Cl-C$_6$H$_4$-CHO	48	4-Cl-C$_6$H$_4$-COOCH$_2$-C$_6$H$_4$-4-Cl	82(1st run) 80(2nd run) 81(3rd run)
11.	Sm[N(SiMe$_3$)$_2$]$_3$	2,3-(MeO)$_2$-C$_6$H$_3$-CHO	24	2,3-(MeO)$_2$-C$_6$H$_3$-COOCH$_2$-C$_6$H$_3$-2,3-(OMe)$_2$	10
12.	S2	2,3-(MeO)$_2$-C$_6$H$_3$-CHO	48	2,3-(MeO)$_2$-C$_6$H$_3$-COOCH$_2$-C$_6$H$_3$-2,3-(OMe)$_2$	5

[a] Yields were determined by GC with an internal standard n-dodecane.

diameter and volume of SBA-15. However, the elemental analyses and IR spectroscopy of S3 suggest that the bound silylamide ligand has been almost replaced by the newly formed alkoxide ligand. This is consistent with the previous proposed pathway for Tishchenko reaction [18].
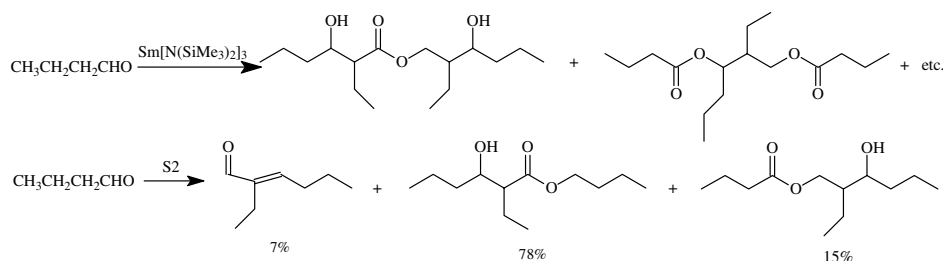
Scheme 2. The reactions of butyl aldehyde catalyzed by $Sm[N(SiMe_3)_2]_3$ and hybrid material (S2).

$$PhCHO + RCHO \longrightarrow PhCO_2CH_2Ph + PhCO_2CH_2R + RCO_2CH_2Ph + RCO_2CH_2R$$

(a)   (b)   (c)   (d)
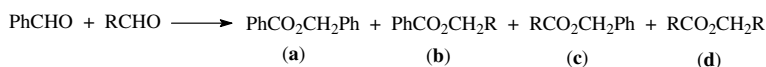
R = fural, 2,3-dimethyoxybenzyl

Scheme 3. Mixed Tishchenko reactions catalyzed by $Sm[N(SiMe_3)_2]_3$ and hybrid material (S2).

Table 2
Selectivity in mixed Tishchenko reactions catalyzed by $Sm[N(SiMe_3)_2]_3$ and hybrid material (S2)

Catalyst	Substrate	Solvent	Time (h)	Selectivity a:b:c:d[a]
$Sm[N(TMS)_2]_3$	PhCHO/furfural (1/1)	Toluene/hexane (1/1)	48	33:36:17:14
S2	PhCHO/furfural (1/1)	Toluene/hexane (1/1)	48	27:53:7:13
$Sm[N(TMS)_2]_3$	PhCHO/2,3-dimethoxybenzaldehyde (1/1)	Toluene/hexane (1/1)	48	49:51:0.3:0
S2	PhCHO/2,3-dimethoxybenzaldehyde (1/1)	Toluene/hexane (1/1)	48	33:67:0:0

[a] Selectivity was determined by GC on the basis of area percentage.

To obtain additional insight into the potential use of the hybrid material in the Tishchenko reaction, we examined the catalytic behavior of S2 toward the mixed Tishchenko reaction (Scheme 3). Significantly, when two kinds of aldehydes (1:1) were utilized in this performance, the yields of the cross products $PhCO_2CH_2R$ in the S2 catalytic system were obviously elevated as compared with the corresponding homogeneous catalysis (Table 2). The change of the selectivity could be attributed to the spatial restriction and the diffusion control of the surface confinement.

3. Conclusions

In summary, we have successfully modified the silicate SBA-15 with samarium silylamide complex, giving a novel hybrid material characteristic for the presence of the reactive metal moieties and the maintenance of the well-ordered mesoporous structure. This new hybrid material $[SBA-15]Sm[N(SiMe_3)_2]_x$ is an efficient and mild catalyst for Tishchenko reaction, especially for mixed Tishchenko reaction it is complementary to the corresponding homogeneous catalyst $Sm[N(SiMe_3)_2]_3$ in selectivity due to the spatial restriction and the diffusion control resulted from the ordered mesoporous structure of the hybrid material. Furthermore, the hybrid material displays greater stability to O_2 compared with $Sm[N(SMe_3)_2]_3$, and it is easily separated from the reaction mixture and can be reused twice at least without significant reduction of activity.

4. Experimental

4.1. General

All syntheses and manipulations of compounds were performed with rigorous exclusion of air and moisture, using high-vacuum and glove-box techniques. Solvents were freshly distilled under argon from Na/K alloy. The dehydrated SBA-15 sample S1 was synthesized according to the literature method [8]. Hexamethyldisilazane was purchased from Aldrich and degassed before use. All aldehydes were obtained from Aldrich and were degassed and stored in glove-box. IR spectra data were obtained with an AUATAR 360 FT-IR (Nicolet) analyzer. Nitrogen adsorption–desorption isotherms were measured with a Micromeritics Tristar 3000 analyzer at 77 K. Samples were degassed prior to analysis under vacuum for 5 h at ambient temperature. The Barrett–Emmett–Teller (BET) method was utilized to calculate the surface areas. The pore volume and pore-size distributions were calculated using the Barrett–Joyner–Halanda (BJH) method.

Powder X-ray diffraction (XRD) patterns were recorded with a Bruker D4 powder X-ray diffractometer using Cu Kα radiation. Elemental analyses were carried out on a Rapid CHN–O analyzer and a S4 EXPLORER X-ray Spectrometer. Gas–liquid chromatograms were performed on a HP 6890 series chromatograph equipped with a FID detector and a HP 5793 mass-spectrometer detector using He as a carrier gas.

4.2. Immobilization of Sm[N(SiMe₃)₂]₃ onto SBA-15

Tris[bis(trimethylsilyl)amido]samarium (0.52 g) was dissolved in *n*-hexane (10 ml), and was quickly added to a suspension of the dehydrated SBA-15 (0.78 g) in *n*-hexane (10 ml). After stirring at ambient temperature for 72 h, the reaction mixture was centrifuged and the solution was decanted. The precipitate was washed several times with *n*-hexane (20 ml) and dried in vacuum for 3 h to give **S2** as a pale-yellow powder. Removal of solvent from the solution left 0.04 g unreacted silylamide.

S1: White powder, BET surface area: 463.7 m²/g. BJH pore diameter: 7.74 nm. IR (KBr): v = 3442 (s), 162s9 (m), 1080 (s), 804 (s) cm⁻¹.
S2: Pale yellow powder, BET surface area: 273.4 m²/g. BJH pore diameter: 6.96 nm. Anal. Found: C, 13.21; H, 3.72; N, 1.96; Sm, 16.1%. IR (KBr): v = 3417 (m), 2964 (m), 1627 (m), 1525 (m), 1392 (m), 1080 (s), 846 (s), 806 (s) cm⁻¹.
S3: Yellow powder, BET surface area: 270.9 m²/g. BJH pore diameter: 6.65 nm. Anal. Found: C, 16.29; H, 1.62; N, 0.48; Sm, 14.6%. IR (KBr): v = 3411 (m), 2964 (m), 2921 (m), 2852 (m), 1594 (m), 1542 (m), 1421 (m), 1087 (s), 804 (m) cm⁻¹.

4.3. General catalytic procedure

The catalytic reactions were carried out under the protection of nitrogen. The qualitative and quantitative analysis of the reactants and the products was made by GLC. Yields were determined by GLC based on the relative area of GLC signals referred to the internal standard (*n*-dodecane). Selectivity is represented by product distribution based on the relative area of GLC signals. Standard lipid products were prepared by the literature procedures [7].

4.3.1. Condensation reactions of aldehydes catalyzed by Sm[N(SiMe₃)₂]₃

The catalyst (2.5 mol% metal) dissolved in *n*-hexane (2 ml) was stirred in a reaction flask. The substrate (0.1 g) dissolved in toluene (2 ml) was directly added to the catalyst. After stirring for 24 h, the reaction mixture was quenched with 2 ml of water, and extracted with CH₂Cl₂ (3 × 2 ml). The combined organic extract
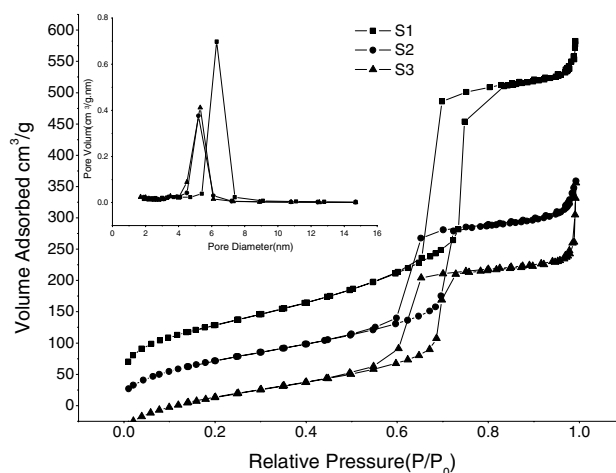

Fig. 3. N₂ adsorption–desorption isotherms at 77 K and pore size distribution profiles of SBA-15 (**S1**), hybrid material (**S2**) and recovered material (**S3**).

was filtered through the MgSO₄ pad. The resulting dry organic layer was then analyzed by GLC.

4.3.2. Condensation reactions of aldehydes catalyzed by the hybrid material

The hybrid material (2.5 mol% metal) suspended in *n*-hexane (2 ml) was stirred in a reaction flask. The substrate (0.1 g) dissolved in toluene (2 ml) was added to the catalyst. After stirring for 24 h, the catalyst was separated from the reaction mixture by centrifugation and washed several times with hexane. The combined organic layer was analyzed by GLC. The recovered material was dried in vacuum and reused for the next run.

4.3.3. Mixed Tishchenko reaction

A mixture of two different aldehydes in 1:1 molar ratio were dissolved in toluene (2 ml) and added to the catalyst in *n*-hexane (2 ml) under the protection of N₂. After the reaction was completed, the mixture was quenched, extracted and analyzed as described above (see Fig. 3).

References

[1] A.D. Pomogailo, I.E. Uflyand, J. Mol. Catal. 55 (1989) 429.
[2] R. Anwander, O. Runte, J. Eppinger, J. Chem. Soc., Dalton Trans. (1997) 137.

[3] R. Anwander, H. Görlitzer, C. Palm, O. Runte, M. Spiegler, J. Chem. Soc., Dalton Trans. (1999) 3611.

[4] D. Zhao, J. Feng, Q. Huo, N. Melosh, G.H. Fredrickson, B.F. Chmelka, G.D. Stucky, Science 279 (1998) 548.

[5] A. Théolier, E. Custodero, A. Choplin, J.M. Basset, F. Raatz, Angew. Chem. Int. Ed. 29 (1990) 805.

[6] (a) G.J. Kim, J.H. Shin, Catal. Lett. 63 (1999) 205;
(b) Y.V.S. Rao, D.E. De Vos, P.A. Jacobs, Angew. Chem. Int. Ed. 36 (1997) 2661;
(c) I. Rodriguez, S. Iborra, A. Corma, F. Rey, J.L. Jordá, Chem. Commun. (1999) 593;
(d) J.V. Walker, M. Morey, H. Carlsson, A. Davidson, G.D. Stucky, A. Butler, J. Am. Chem. Soc. 119 (1997) 6921.

[7] T. Ooi, T. Miura, K. Takaya, K. Maruoka, Tetrahedron Lett. 40 (1999) 7695.

[8] O.P. Tormakangas, P. Saarenketo, A.M.P. Koskinen, Org. Process Res. Dev. 6 (2002) 125.

[9] (a) T. Seki, K. Akutsu, H. Hattori, Chem. Commun. 11 (2001) 1000;
(b) T. Seki, H. Hattori, Chem. Commun. 23 (2001) 2510;
(c) T. Seki, H. Kabashima, K. Akutsu, H. Tachikawa, H. Hattori, J. Catal. 204 (2001) 393;

(d) T. Seki, H. Tachikawa, T. Yamada, H. Hattori, J . Catal. 217 (2003) 117.

[10] H. Berberich, P.W. Roesky, Angew. Chem. Int. Ed. 37 (1998) 1569.

[11] D. Zhao, Q. Huo, J. Feng, B.F. Chmelka, G.D. Stucky, J. Am. Chem. Soc. 120 (1998) 6024.

[12] R. Anwander, I. Nagl, M. Widenmeyer, J. Phys. Chem. B 104 (2000) 3532.

[13] M. Jia, A. Seifert, W.R. Thiel, Chem. Mater. 15 (2003) 2174.

[14] R. Anwander, Chem. Mater. 13 (2001) 4419.

[15] A. Stein, M.H. Lim, Chem. Mater. 11 (1999) 3285.

[16] G. Gerstberger, C. Palm, R. Anwander, Chem. Eur. J. 5 (1999) 997.

[17] (a) D. Rohan, C. Canaff, E. Fromentin, M. Guisnet, J. Catal. 177 (1998) 296;
(b) M.C. Hausladen, R.C. Cyganovich, H.Y. Huang, C.R.F. Lund, Appl. Catal. 219 (2001) 1;
(c) X. Wu, M.G. Abraha, R.G. Anthony, Appl. Catal. 260 (2004) 63.

[18] S. Onozawa, T. Sakakura, M. Tanaka, M. Shiro, Tetrahedron 52 (1996) 4291.